Rossby wave interactions with Mediterranean and subtropical latitudes

Dominique Lambert, Jean-Pierre Cammas

Rossby wave interactions with Mediterranean and subtropical latitudes

Dominique Lambert · Jean-Pierre Cammas

Abstract The downstream influence of a Rossby wave on weather conditions in the Mediterranean and North Africa is studied. The objective is to gain a better understanding of the atmospheric processes in these regions and to improve their quantification. The emphasis is placed on high-impact weather events to improve numerical forecasts and warnings about these hazardous weather phenomena. For this purpose, 4 days from 5 to 8 February 1997 are used to investigate both a Mediterranean low and a subtropical African convective situation. Sensitivity studies, using a potential vorticity inversion tool associated with the French atmospheric model ARPEGE, are presented. The Mediterranean surface low under study is shown to be associated with the mid-latitude upper level potential vorticity anomaly, itself associated with a Rossby wave. A subtropical convective cell is shown to be related to upward vertical motions associated with a cut-off low; this cut-off low coming from a mid-latitude Rossby wave.

1 Introduction

Rossby waves are defined by Holton (1992) in these terms: "in a baroclinic atmosphere, the Rossby wave is a potential-conserving motion that owes its existence to the isentropic gradient of potential vorticity (PV)". For Stull (2000), "if some small disturbance causes the jet stream blowing from west to east at mid-latitudes to turn slightly northward, then conservation of PV causes the jet to meander north and south. This meander of the jet stream is called a Rossby wave or planetary wave". Rossby wave energy propagation is an important feature of the general atmospheric circulation. For example, mid-latitude cyclogenesis can be associated with this phenomenon. Thus, it is of great importance for weather forecasting accuracy. Over the north Atlantic, cyclogenesis was studied during the Fronts and Atlantic Storm Track Experiment (FASTEX) programme set up to make detailed observations of extratropical cyclones reaching the west coast of Europe (Joly et al. 1999). One of the objectives was the investigation of upper tropospheric dynamics to explain mid-latitude cyclogenesis. In particular, PV studies were conducted to synthesise these explanations. For example, Lambert et al. (2004) used PV inversion techniques and model simulations to study a FASTEX cold air cyclogenesis. Likewise, Moore et al. (2008a) used the same approach to study a heavy snowfall event in the north-eastern United States. Moreover, the Mesoscale Alpine Program (MAP) (Bougeault et al. 2001) studies have shown that meteorological situations leading to heavy Alpine south-side precipitation are often associated with an upper level trough, oriented north–south and located over Spain and France. Such an upper level anomaly corresponds to an intrusion of stratospheric air and is characterised by high PV values. The spatio-temporal evolution of precipitation is conditioned by the geographical situation of this high level anomaly, its eastward advection speed and its internal structure (Fehlmann and Quadri 2000). The importance of PV filaments in the spatio-temporal distribution of precipitation has been confirmed by Hoinka et al. (2003), and Liniger and Davies (2003), on an intense precipitation case during MAP. Likewise, Donnadille et al. (2001a) have documented the life cycle of a tropopause fold combined with the development of a FASTEX low. The folding can

D. Lambert (✉) · J.-P. Cammas
Laboratoire d'Aérologie, Université de Toulouse,
CNRS, 14 av. Edouard Belin, 31400 Toulouse, France
e-mail: dominique.lambert@aero.obs-mip.fr

be found when a severe quasi-horizontal distortion of PV occurs, called "planetary wave breaking" or Rossby wave breaking (RWB). The first detailed observational evidence of RWB in the stratosphere was provided by McIntyre and Palmer (1983). RWB is characterised by the rapid (of the order of a day) and irreversible deformation of material contours (Postel and Hitchman 1999). McIntyre and Palmer (1983) describe the RWB as "a phenomenon ubiquitous in nature and arguably one of the most important dynamical processes affecting the stratosphere as a whole". RWB is an important contributor to the complex of mixing processes in the atmosphere. As recalled by Allen et al. (2009), RWB and associated tropopause folds are ubiquitous features of upper tropospheric meteorology and are reasonably well understood theoretically. Less well understood is the influence of folds on lower level dynamics, especially their ability to modulate convection. For example, Kiladis (1998) presents observations of Rossby waves linked to convection over the Eastern Tropical Pacific. Moore et al. (2008b) examine the dynamical role of downstream development associated with Kona low genesis. Allen et al. (2009) examine the role of RWB generated along the Southern Hemisphere subtropical jet stream on the distribution of deep convection over north-west Australia.

In the same way, interactions between mid-latitudes and Mediterranean or subtropical latitudes are discussed in several papers. For instance, Knippertz and Martin (2005) present a relation between PV streamers and tropical plumes and extreme precipitation in subtropical and tropical West Africa. These PV streamers are formed as a result of an equatorward transport of high-PV air downstream of a large ridge over the North Atlantic. Another example for north-west Africa is the study by Knippertz and Martin (2007). Their observational study addresses the role of dynamic and diabatic processes in the generation of cut-off lows over north-west Africa. They state that more quantitative dynamical and statistical studies are needed to better understand the relative contributions of single factors to the large and synoptic scale evolution that leads to PV streamers and cut-offs near West Africa. Similarly, other studies focus on the Alpine (Lanzinger 1992; Massacand et al. 1998, 2001; Hoinka et al. 2003) and Mediterranean regions. At the Mediterranean basin scale, Buzzi et al. (2003) show that the atmospheric humidity content may depend on the lower level flow and can be influenced by orography (Alps, Pyrenees, Atlas). Lebeaupin et al. (2006) present sensitivity of torrential rain events in the South of France to the Mediterranean Sea surface temperature. Moreover, links between upper level structures and heavy rainfall events and/or cyclogenesis in the Mediterranean are also investigated in several papers. Some examples are mentioned below. Prezerakos et al. (1999) demonstrate that the upper tropospheric downstream development could be closely related to the upper tropospheric frontogenesis that appears upon the north-eastern flank of a blocking high. Kurz and Dalla Fontana (2004) present a case of cyclogenesis over the western Mediterranean Sea with large amount of latent heat released in the condensation process, which produces significant modifications of the flow. Basset and Ali (2006) investigate several aspects of a Mediterranean cyclogenesis within a PV framework. Porcù et al. (2007) introduce a classification of cut-off episodes in the Mediterranean region, based on the vertical extension of the depression and the presence of a linked surface vortex also analysing precipitation patterns. Krichak et al. (2007) present a case study in which a powerful PV streamer system played a major role in the process over the south-eastern Mediterranean region. Lagouvardos et al. (2007) performed sensitivity tests at the meso scale using a model and PV inversion, showing that the upper level dynamic forcing was the main factor that led to the studied explosive cyclogenesis over the Aegean Sea. Argence et al. (2008) study the impact of initial condition uncertainties on the predictability of heavy rainfall in the Mediterranean. Kaspar and Müller (2009) present a study aimed at diagnosing cyclogenesis in the Mediterranean basin using synoptic-dynamic anomalies. Argence et al. (2009) show that PV corrections lead to a substantial improvement in the simulation of a Mediterranean storm at the meso scale, in terms of surface pressure, cloud cover and precipitation forecasts. Claud et al. (2010) were interested on the impact of fine-scale upper level structures on the deepening of a Mediterranean "hurricane".

These few papers show the importance of having a better understanding and quantification of the atmospheric processes in the Mediterranean and North Africa, with emphasis on high-impact weather events to improve numerical forecasts and warnings about these hazardous weather phenomena. Although the PV inversion method is increasingly used in research, forecasters need a maximum of studies to strengthen their approach in operational forecasting.

The present paper is part of this approach. Two case studies allow the investigation of both Mediterranean cyclogenesis and cut-off low formation north-west of Africa in February 1997 during FASTEX. This period has benefited from improved analysis taking into account additional data from FASTEX (Desroziers et al. 1999, 2003). It has already been studied by Kowol-Santen et al. (2000) to estimate the cross-tropopause airmass fluxes at mid-latitudes. Here, a high level anomaly associated with a Rossby wave is first studied in relation with the occurrence of a Mediterranean cyclone. Then, links between tropical convective forcing and the vorticity advection during a cut-off low formation are considered. The paper is structured as

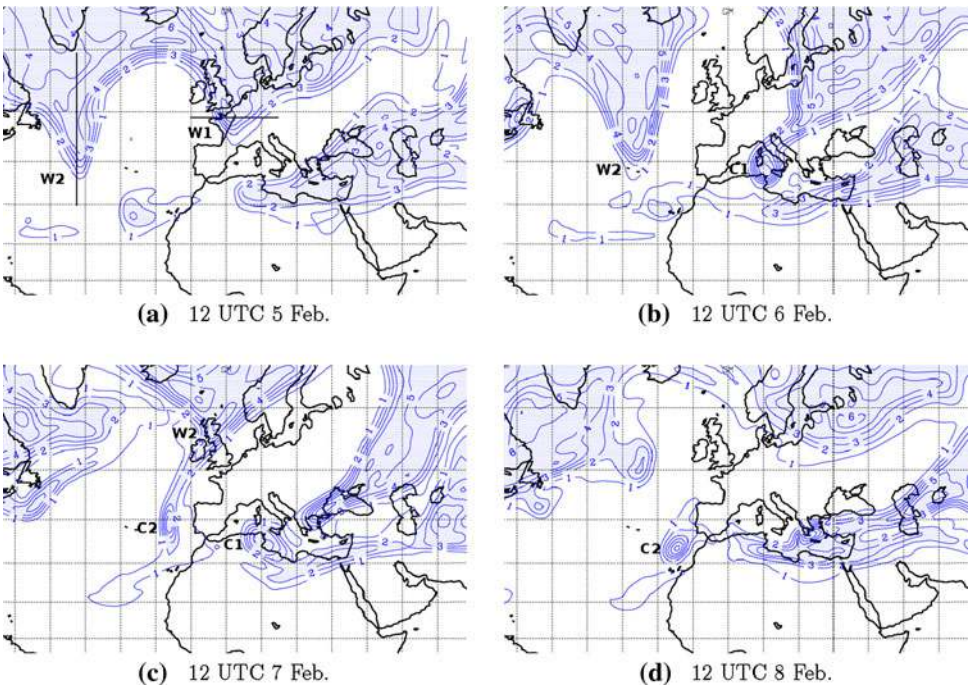

Fig. 1 300 hPa PV reanalyses (every 1 pvu, shaded from 2 pvu) for **a** 5 February 1200 UTC, **b** 6 February 12 UTC, **c** 7 February 1200 UTC and **d** 8 February 1200 UTC. *Bold lines* in **a** correspond to the locations of Figs. 5, 7, and 12 vertical sections. GM is for Greenwich Meridian. *W1*, *W2* tips of main waves, *C1*, *C2* corresponding cut-off lows

follows: in Sect. 2, the methodology and the situation studied are described. In Sect. 3, a sensitivity test using a PV inversion tool is applied to Mediterranean cyclogenesis. In Sect. 4, this PV inversion tool is used to show the relationship between a convective cell north-west of Africa and a cut-off low arising from the Rossby wave.

2 Methodology and situation description

2.1 Methodology

Piecewise PV inversion has been applied in numerous studies to investigate the effect on the forecast fields of modifying the PV perturbations in the model initial conditions (Hello and Arbogast 2004; Lambert et al. 2004; Lagouvardos et al. 2007; Argence et al. 2009; Claud et al. 2010). This technique is based on the PV invertibility principle (Hoskins et al. 1985) and was initially proposed by Davis and Emanuel (1991). The principle of manipulating initial conditions through quasi-geostrophic potential vorticity and the PV inversion tool are presented in Chaigne and Arbogast (2000). In the version used for this study, we do not solve the omega equation. After PV inversion, the ARPEGE model is used to perform adjustments during the first steps. A potential drawback of this method is that, during the adjustment phase, the initial perturbation is modified. As we will see, this weakness is not harmful for this study. Other recent methods exist, such as the method in which a divergent wind perturbation is built without the omega equation (Arbogast et al. 2008).

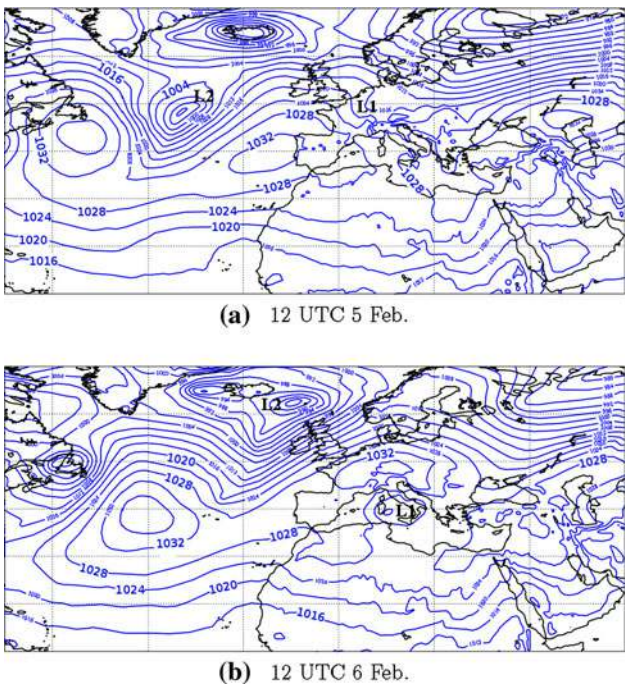

Fig. 2 Mean sea level pressure (hPa), every 4 hPa for **a** 5 February 1200 UTC and **b** 6 February 1200 UTC. L1 and L2 correspond to surface lows involved in this study

The spectral operational model ARPEGE (Action de Recherche Petite Echelle et Grande Echelle) (see Courtier et al. 1991 for more details) is run with T95 spectral resolution (which corresponds to about two degrees in the North Atlantic) and 27 vertical levels. All plots presented hereafter use this resolution. All the reanalyses used in the

present study include FASTEX data. The FASTEX special data (soundings, aircraft and ship measurements, etc.) were added to the conventional data set and assimilated into a four-dimensional variational scheme (see Desroziers et al. 1999, 2003 for details). The noteworthy quality of these reanalyses is one of the reasons that guided the choice of this study. Hereafter, an experiment in which some PV is removed or modified will be called a "modified" experiment. The PV inversion tool was implemented using the following strategy. Two simulations were performed with identical model tuning except for the initial conditions. The initial conditions for the first simulation (reference) were standard ARPEGE reanalyses. Initial conditions for the second simulation were obtained from a PV surgery method following Chaigne and Arbogast (2000). PV surgery was performed in three steps. First, the ARPEGE reanalyses were examined to locate subjectively interesting PV structures. Second, these identified structures were removed. Finally, the PV inversion tool was used to retrieve modified velocity and temperature fields corresponding to the modified PV field. While some studies mention the possibility of addressing relationships between dynamics and moisture through PV inversion (McTaggart-Cowan et al. 2003; Arbogast et al. 2008), the PV inversion technique used in this study (as in Funatsu and Waugh (2008)) cannot determine the amount of moisture directly associated with a particular distribution of PV.

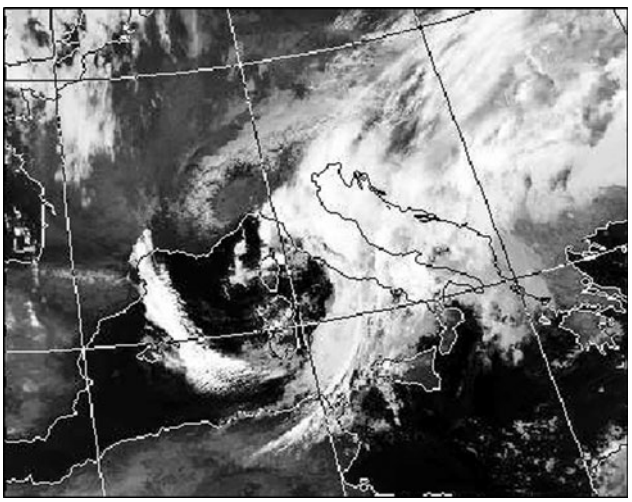

Fig. 3 AVHRR longwave cloud image (NOAA 14 satellite) at 0142 UTC 6 February 1997 (from http://www.sat.dundee.ac.uk)

2.2 Situation studied

Figure 1 presents 300 hPa PV reanalyses every 24 h from 5 February 1200 UTC to 8 February 1200 UTC 1997. The threshold value [2 pvu (1 pvu $= 10^6$ K m^{-2} s^{-1} kg^{-1})] for the shading corresponds approximately to the dynamic tropopause. The shaded area locates the stratosphere. Two main characteristics can be seen in Fig. 1: a mid-latitude wave and an approximately zonal structure more or less stretched to the south. On 5 February 1200 UTC (Fig. 1a), the mid-latitude waving aspect is clear: between approximately 40 N and 60 N, the 300 hPa PV shape corresponds to a succession of troughs and highs. The southern tips of the two main troughs are located approximately 2 E (W1) and 42 W (W2) between 35 N and 45 N. From 5 February 1200 UTC to 8 February 1200 UTC, these two waves propagate eastwards. South of this wave, an elongated quasi-zonal PV structure extending approximately from 25 N to 35 N and from 30 W to 30 E is present on 6 February 1200 UTC (Fig. 1b). Further to the east, this structure is stretched northwards. The 1 pvu isoline clearly shows this elongated structure. This zonal elongated structure is located at the cyclonic-shear side of the subtropical jet. On 5 February 1200 UTC, we can consider that this structure was already present but not represented because of the low resolution of the reanalyses. On 7 February 1200 UTC (Fig. 1c), this zonal structure is fed by W2 which is being transformed into the C2 cut-off low. An intense PV maximum (5 pvu) is located over the

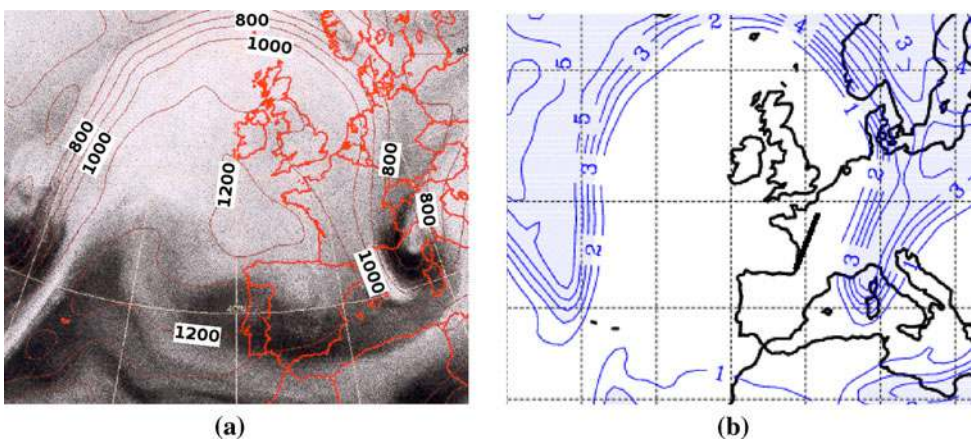

Fig. 4 **a** Meteosat water vapour image at 0000 UTC 6 February superimposed with the 2 pvu geopotential high (×10 m). **b** 300 hPa PV reanalysis (every 1 pvu, shaded from 2 pvu) for 6 February 0000 UTC. *Bold line* corresponds to the location of the vertical section of Fig. 5

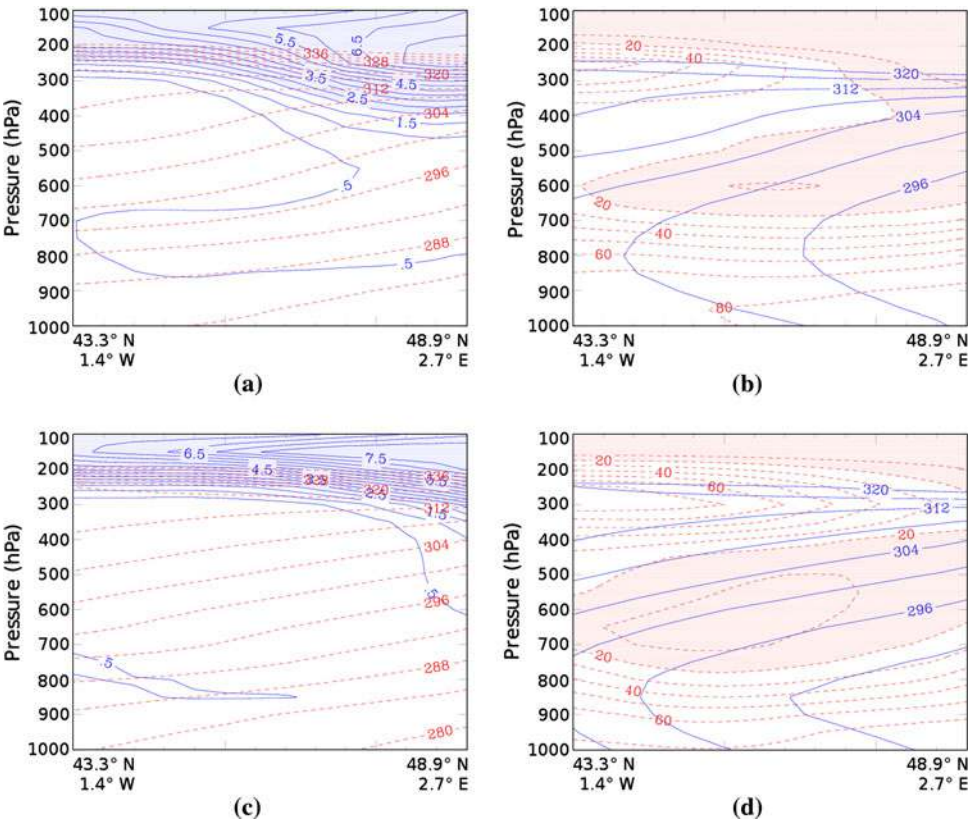

Fig. 5 **a**, **c** Vertical sections of PV (*solid lines*) shaded from 2 pvu (every 0.5 pvu) and potential temperature (dashed lines, every 4 K, up to 340 K). **b**, **d** Vertical sections of equivalent potential temperature (solid lines, every 4 K, up to 340 K) and relative humidity (*dashed lines*, every 10%, shaded from 0 to 20%). **a**, **b** 5 February 1200 UTC. **c**, **d** 5 February 1800 UTC

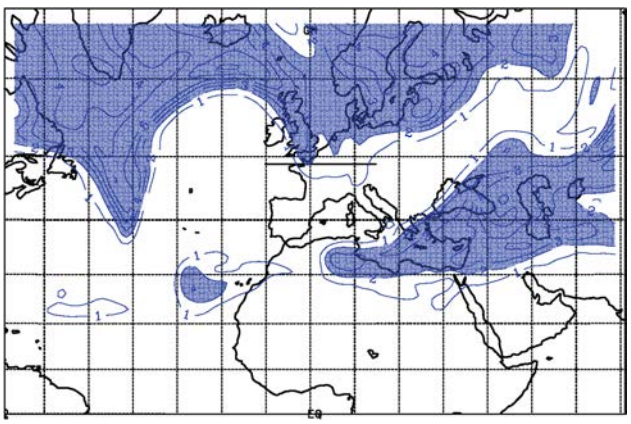

Fig. 6 300 hPa PV (every 1 pvu, shaded from 2 pvu) modified with the inversion tool for 5 February 1200 UTC. *Bold line* corresponds to the location of the vertical section of Fig. 7. GM is for Greenwich Meridian. EQ is for Equator

Mediterranean at approximately 10 E 35 N (C1 on Fig. 1c). This maximum seems to have its origin in W1 as shown in Fig. 1b, where W1 presents a quasi-cut-off low (PV maximum of 6 pvu already called C1) located 10 E 37 N. On 8 February 1200 UTC (Fig. 1d), another high-PV value isolated structure is located north-west of Africa (approximately 15 W 34 N). This cut-off low (C2), characterised by a maximum of 6 pvu seems to have its origin in W2. Indeed, 24 h earlier (Fig. 1c) there is a quasi meridional structure from W2 (5 W 55 N) to C2 (17 W 38 N).

Figure 2 presents the mean sea level pressure (MSLP) field on 5 February 1200 UTC and 6 February 1200 UTC. Two main characteristics are of particular interest for our study. First, a surface low (L1) begins to form on 5 February 1200 UTC (Fig. 2a), east of France. 24 h later (Fig. 2b), it is characterised by an isolated relative minimum MSLP isoline (1,020 hPa called "a low" below by misuse of language) located east of Sardinia (10 E 39 N). Second, and further west, an isolated 992 hPa surface low (L2) is located 33 W 49 N on 5 February 1200 UTC (Fig. 2a). This low was well documented during one of the FASTEX Intensive Observing Periods (IOP 11) (Joly et al. 1999). 24 h later, this surface low has deepened to reach 972 hPa. It is located 10 W 62 N on 6 February 1200 UTC (Fig. 2b). Other surface lows and ridges appear on Fig. 2 but they are not involved in our study.

By analysing Figs. 1 and 2 together, we can see that W1 and W2 dynamics variations seem to be associated with those of L1 and L2. W1 and W2 are positioned upwind of L1 and L2, respectively. This organisation corresponds to the classic barocline interaction mechanism for maintaining and reinforcing a surface low (Charney 1947; Hoskins et al. 1985). These two associated structures will be studied below using the PV inversion tool in association with the ARPEGE model as explained in Sect. 2.1.

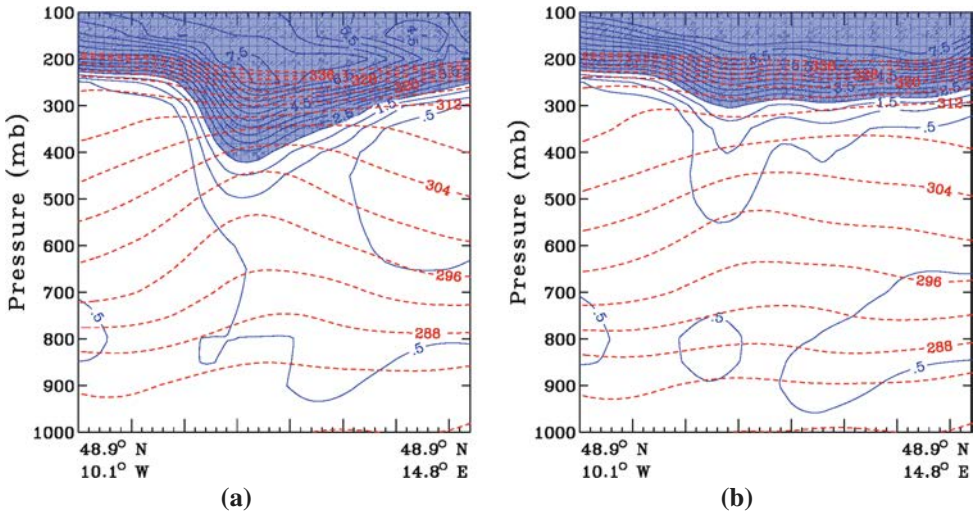

Fig. 7 Vertical sections of PV (*solid lines*, shaded from 2 pvu, every 0.5 pvu) and potential temperature (*dashed lines*, every 4 K, up to 340 K) for 5 February 1200 UTC. **a** Reanalyses (initial time of S1); **b** "Modified" state (initial state of S2)

3 Mediterranean cyclogenesis

As mentioned in the introduction, Mediterranean cyclogenesis is sometimes associated with intense weather conditions: high winds (Jiang et al. 2003), convective activity (Kurz and Dalla Fontana 2004) which can induce catastrophic material damage and sometimes casualties. In this study, from 6 February 1200 UTC to 7 February 0000 UTC, the MSLP fields show an isolated relative minimum being advected from the south-east of France to Tunisia during the period (not shown). Figure 3 presents a long-wave picture from the AVHRR radiometer onboard the NOAA 14 satellite on 6 February 0142 UTC. The surface low roughly located over Corsica is characterised by a cloudy vortex structure, which is in agreement with reanalyses of Fig. 2 (note that the time of the satellite picture is between Fig. 2a, b). Figure 4a presents the water vapour picture from the Meteosat satellite superimposed with the 2 pvu geopotential high on 6 February 0000 UTC. The dark area extending from the west of Sardinia to the west of Switzerland corresponds to a dry stratospheric air intrusion over the Mediterranean Sea, west of Corsica and Sardinia, which is in agreement with the 300 hPa PV field distribution shown in Fig. 4b. This satellite information validates the high quality of the reanalyses.

Figure 5 presents vertical sections over France from approximately Biarritz to Paris of, on the left, PV and potential temperature and, on the right, relative humidity and equivalent potential temperature. PV values greater than 2 pvu are shaded. Figure 5a, b is for 5 February 1200 UTC. Figure 5c, d is for 5 February 1800 UTC. The 2 pvu altitude is 250 hPa at 43.3 N, south of this section approximately over Biarritz, and 400 hPa at 48.9 N over Paris in Fig. 5a. In consequence, the tropopause given by the ARPEGE reanalyses is higher over Biarritz than over Paris. The lowering of the tropopause towards the north corresponds to the interception of W1 (see Fig. 1a). On 5 February 1800 UTC (Fig. 5c), the tropopause altitude is much more constant and, at 1800 UTC, W1 has been advected eastwards and is not intercepted in the vertical section of Fig. 5c. Figure 5b, d presents relative humidity and equivalent potential temperature vertical sections approximately from Biarritz to Paris for 1200 UTC and 1800 UTC respectively. Relatively dry stratospheric air masses (relative humidity lower than 20%) penetrate into the troposphere at 1200 UTC (Fig. 5b). Keeping in mind that we are using reanalyses, quite good agreement is found between PV (if the 0.5 pvu isoline is considered in Fig. 5a) and relative humidity (lower than 20% in Fig. 5b). This drying approximately from 750 to 450 hPa is slightly increased (with a 10% relative humidity kernel at around 600 hPa) from 1200 UTC (Fig. 5b) to 1800 UTC (Fig. 5d) on 5 February whereas the PV anomaly has moved towards the east and it is practically absent from the vertical section for 5 February 1800 UTC (Fig. 5d). This drying appears to be more stationary than the dynamics.

In the previous section, we assume that the interpretation of Figs. 1 and 2 rightly takes the interaction between high atmospheric levels and the surface as a probable key factor. Furthermore, the good quality of the reanalyses has been confirmed by satellite images. Now we propose to test the influence of the high level PV structure (W1) on the surface low (L1) by removing the upper feature using a PV inversion tool together with a set of two ARPEGE simulations (S1 and S2) as described in Sect. 2. The initial time of S1 and S2 is 5 February 1200 UTC. Figure 1a corresponds to the reference initial state of simulation S1 while Fig. 6 is the initial state of simulation S2, which corresponds to an attenuation of W1 over France. This attenuation consists of subjectively choosing an atmospheric volume in which the PV inversion is applied. This volume is defined to best adjust the PV anomaly. Figure 7 presents

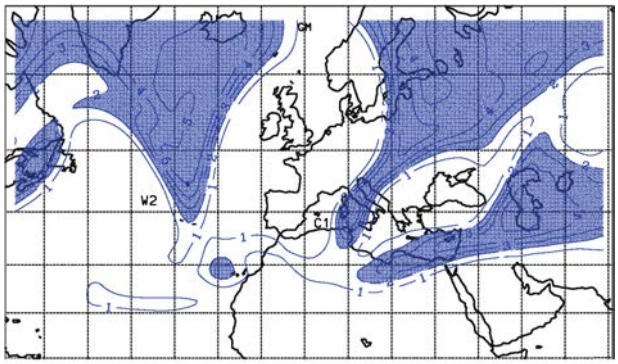

(a)

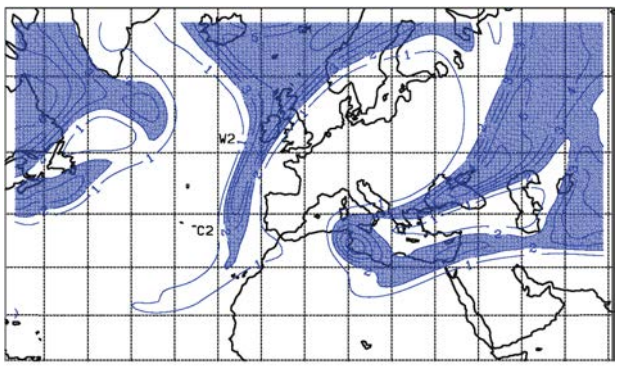

(b)

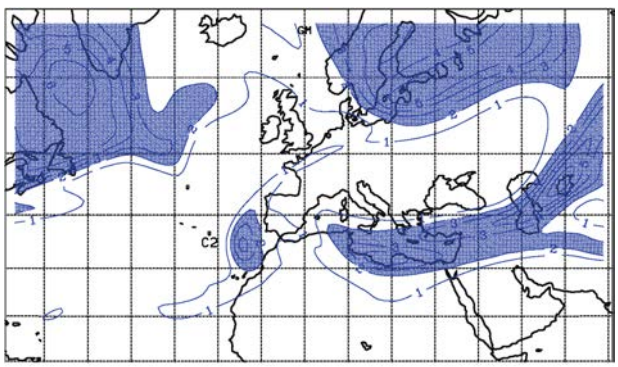

(c)

Fig. 8 300 hPa PV (every 1 pvu, shaded from 2 pvu) for the **a** 24-h, **b** 48-h and **c** 72-h reference simulation (S1) initialized on 5 February 1200 UTC valid, respectively, on 6 February 1200 UTC, 7 February 1200 UTC and 8 February 1200 UTC. W1, W2, C1, C2 as in Fig. 1. GM is for Greenwich Meridian

zonal vertical sections of PV and potential temperature across the north of France. Figure 7a is the reference initial state for S1. Approximately in the middle of the section, the PV anomaly corresponding to high PV values in the troposphere associated with cooling is present. Figure 7b is the modified initial state for S2. Comparison of Fig. 7a, b shows that the attenuation of the anomaly is well represented. Even though the 1 pvu isoline presents a small anomaly, it only reaches 400 hPa in the modified initial

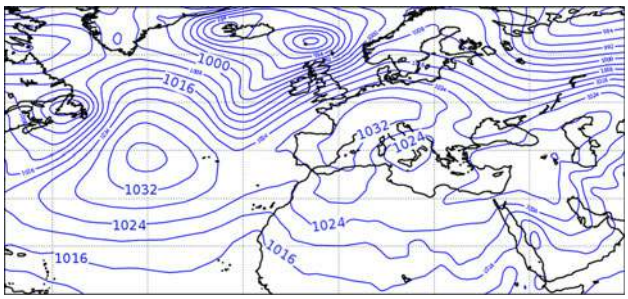

Fig. 9 Mean sea level pressure (every 4 hPa) for the 24-h reference simulation (S1) valid on 6 February 1200 UTC

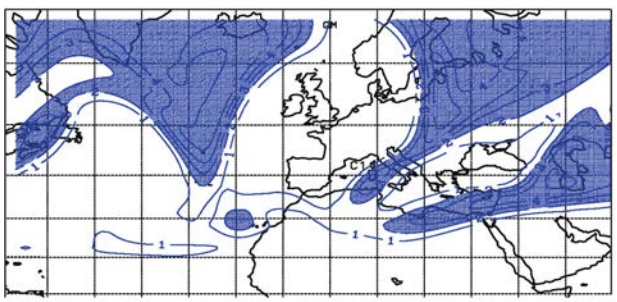

(a)

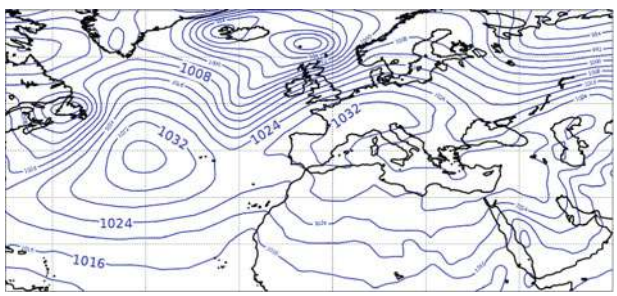

(b)

Fig. 10 24-h "modified" simulation S2 valid on 6 February 1200 UTC for **a** 300 hPa PV (every 1 pvu, shaded from 2 pvu) (GM is for Greenwich Meridian and C1 as in Fig. 1) and **b** the mean sea level pressure (every 4 hPa)

state whereas it reaches 500 hPa in the reference initial state. For higher PV values, this is more obvious with quasi-horizontal isolines in the modified initial state where there was an anomaly in the reference state. Simulations S1 and S2 are two 72-h ARPEGE simulations that differ only by their initial state as described above. In a first step, the reference ARPEGE simulation (S1) was evaluated. This 72-h simulation began on 5 February 1200 UTC. Figure 8 presents results of the 24, 48 and 72-h simulations for the 300 hPa PV. This reference simulation is in agreement with the reanalyses (Fig. 1): W1, W2, C1 and C2 are well located. However, there is a small under-estimation of the simulated 300 hPa PV intensity. For example, maximum 300 hPa PV for C2 on the 72-h simulation valid on 8

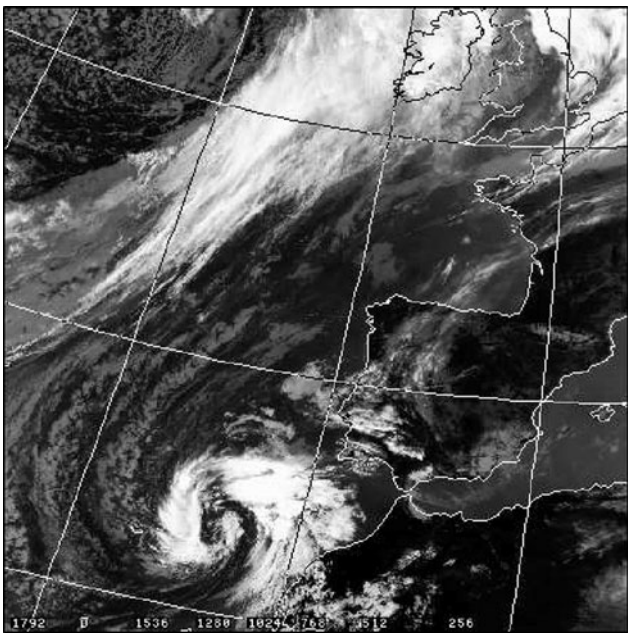

Fig. 11 AVHRR longwave cloud image (NOAA 14 satellite) at 1437 UTC on 8 February 1997 (from http://www.sat.dundee.ac.uk)

February 1200 UTC is 4 pvu whereas it is 6 pvu for the reanalysis at the same date. Nevertheless, the principal characteristics for our study are well reproduced by S1. Figure 9 presents the MSLP 24-h reference simulation (S1) valid on 6 February 1200 UTC. As for the PV, when comparing Fig. 9 with Fig. 2b, we can conclude that S1 is in good agreement with the corresponding reanalyses: this agreement is very good for the location of the surface low L1, and there is a small under-estimation (4 hPa for the MSLP) of its amplitude. Therefore, a comparative study between the reference simulation and simulations with modified initial states using the PV inversion tool is possible.

Figure 10a, b presents, respectively, the 300 hPa PV and MSLP 24-h simulation valid on 6 February 1200 UTC for the modified simulation S2. On comparing S1 and S2 for the 24-h simulation of 300 hPa PV (Figs. 8a, 10a, respectively), we can see that there is no modification in location but C1 is lower in S2 than in S1 (maximum value of 3 pvu for C1 in S2 compared to 5 pvu for C1 in S1). The consequence for cyclogenesis is the non-formation of the closed Mediterranean low (L1) east of Sardinia in the modified forecast S2 (Fig. 10b compared to Fig. 9).

4 Convective cell and cut-off low north-west of Africa

This part deals with the second wave (W2) of the Rossby wave case study. Figure 11 presents the long-wave satellite image for 8 February 1200 UTC over the western part of Europe, North Africa, and near the Atlantic Ocean. In spite of the time gap (2 h 37 min) between the satellite image and the reanalysis, the convective cells located north-west of Africa and the cut-off low (C2) on Fig. 1d are quasi co-located. The aim of this study is to understand the presence of this convective phenomenon by looking for possible coupling with the larger scale meteorological situation. This section presents a sensitivity study of W2 to C2.

A modification of W2 using the PV inversion tool on 5 February 1200 UTC was tested. Figure 12a presents a PV and potential temperature vertical section from 59.5 N, 42.5 W to 29.8 N, 42.5 W across W2 for 5 February 1200 UTC. A clearly distinct anomaly characterised by an intrusion of stratospheric air (high PV values) into the troposphere and local cooling is shown. Figure 12b presents the same vertical section after use of the PV inversion tool as presented above. The set-up of this experiment is comparable to the previous one. Only the horizontal and vertical extent has been adjusted. While in the reference reanalysis (Fig. 12a), the 1 pvu isoline reaches the 750 hPa level, in the modified analysis, the tropopause is quasi horizontal (without anomaly) above 400 hPa. This modified analysis is now used as an initial state for a new 72-h ARPEGE simulation (S3). S3 differs from S1 only by the initial state near W2. Figure 13 presents the 300 hPa PV

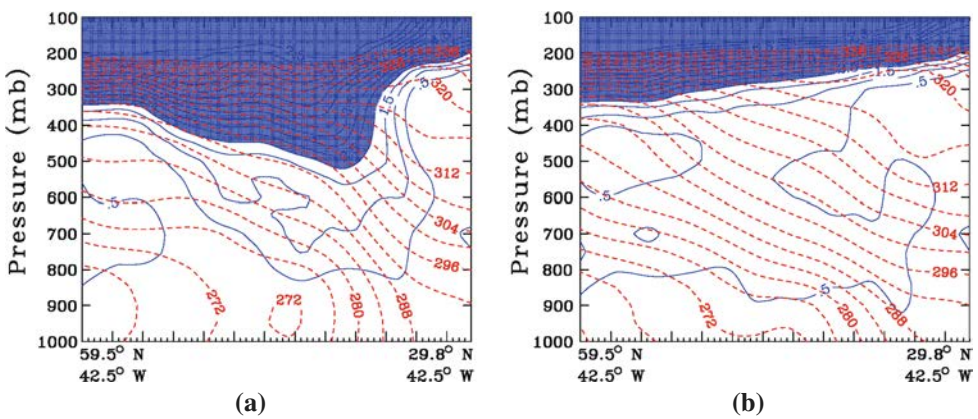

Fig. 12 Vertical sections of PV (*solid lines*, shaded from 2 pvu, every 0.5 pvu) and potential temperature (*dashed lines*, every 4 K, up to 340 K) for 5 February 1200 UTC. **a** Reanalyses; **b** "modified" state

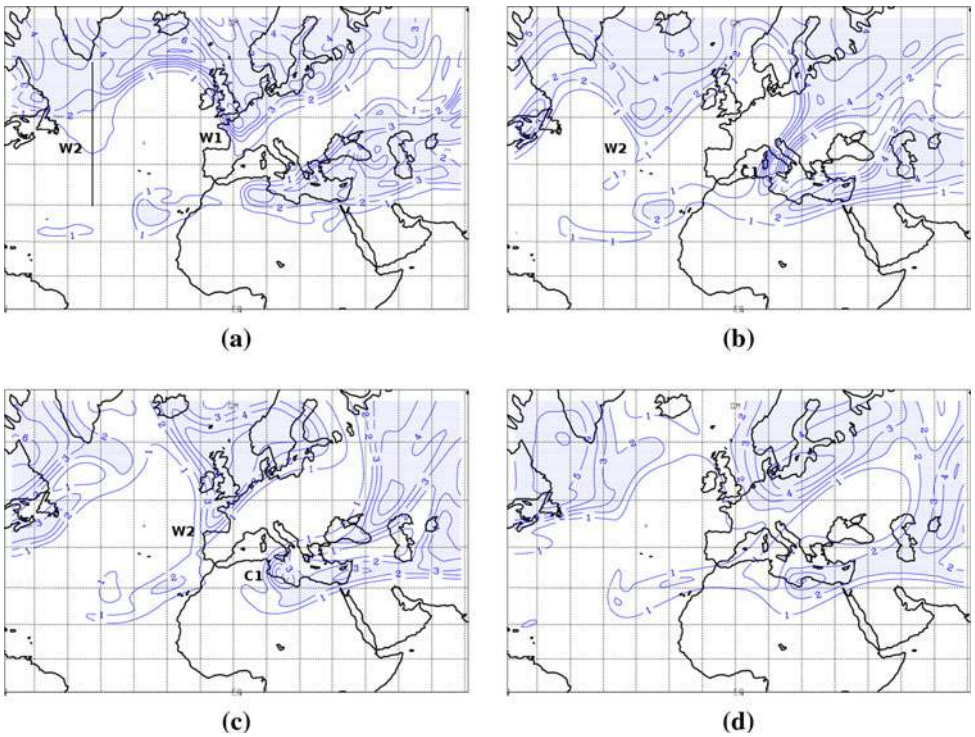

Fig. 13 300 hPa PV (every 1 pvu, shaded from 2 pvu) for the 72-h "modified" simulation (S3) every 24 h valid on 5 February 1200 UTC (**a**), 6 February 1200 UTC (**b**), 7 February 1200 UTC (**c**) and 8 February 1200 UTC (**d**). *Bold line* in **a** corresponds to the location of the vertical sections of Fig. 12b. *W1*, *W2* tips of main waves; *C1* cut-off low associated with W1. GM is for Greenwich Meridian

every 24 h of this new simulation. At the initial state (Fig. 13a), only W2 is reduced; other characteristics are not modified, in particular C2 north-west of Africa. However, even if W2 is reduced at the initial time, it is still present in each step of the simulation. Its longitude location is comparable with S1 but it differs in amplitude and in southward extension. Unlike in S1, in S3 there is no interaction between W2 and C2. In the reference 48-h simulation S1 (Fig. 8b), a PV filament linking W2 and C2 appears. This is in agreement with the reanalysis (Fig. 1c). In contrast, this characteristic is reduced for S3 (Fig. 13c). Consequently, C2 is not modified in S3: it conserves a 2 pvu 300 hPa PV maximum in S3 whereas it is 4 pvu in the reference forecast S1. With this sensitivity study, a coupling between the mid-latitude Rossby wave and the subtropical latitude cut-off low deepening is shown. It seems that mid-latitude stratospheric air plays the role of a reservoir to reinforce the subtropical cut-off low. When the link between the two is made (simulation S1) the cut-off low deepens; when this is not the case (simulation S2), the cut-off low does not evolve.

The cyclonic shape of the cloud structure shown by the satellite image at about midday on 8 February 1997 (Fig. 11) suggests the presence of a surface low associated with convective cells. These convective cells are characterised by intense ascending motion. Figure 14 presents a diagnostic computation of vertical velocity fields performed using the alternative balance (AB) omega equation (Davis-Jones 1991; Mallet et al. 1999; Donnadille et al. 2001b; Lambert et al. 2004). Based on the geostrophic momentum approximation, the AB omega equation keeps the formalism of the quasi-geostrophic omega equation by approximating the horizontal and vertical derivatives of the wind by those of the non-divergent and geostrophic winds respectively. As mentioned by Davis-Jones (1991), the AB approximation implies that thermal-wind balance is restored instantaneously by the secondary circulations and filters inertial gravity waves. It preserves the correct form of the vortex stretching term and it makes the hypothesis less restrictive for the size of the diagnosed movements. The linearity of the omega equation allows the vertical velocity shown on Fig. 14 to be derived. Figure 14a presents the 500 hPa AB vertical wind field for 8 February 1200 UTC from ARPEGE reanalyses. An easily distinguishable ascending vertical wind core (-0.6 Pa s^{-1}) is located at approximately 12 W 32 N. Approximately 5° to the west, there is a subsiding vertical core ($+0.6$ Pa s^{-1}). These two cores form a vertical motion dipole which could be associated with the cut-off low C2 (characterised by 1 pvu isoline reaching 650 hPa, not shown) with ascending motion downwind and subsiding motion upwind of the cut-off low. This is the typical vertical wind pattern that one expects to be linked to all positive upper level PV anomalies (Hoskins et al. 1985; Knippertz and Martin 2005; Funatsu and Waugh 2008). The penetration depth of the upper level disturbance associated with a decrease in the static stability (not shown) is slightly deeper than in the Funatsu and Waugh (2008) case study. As mentioned

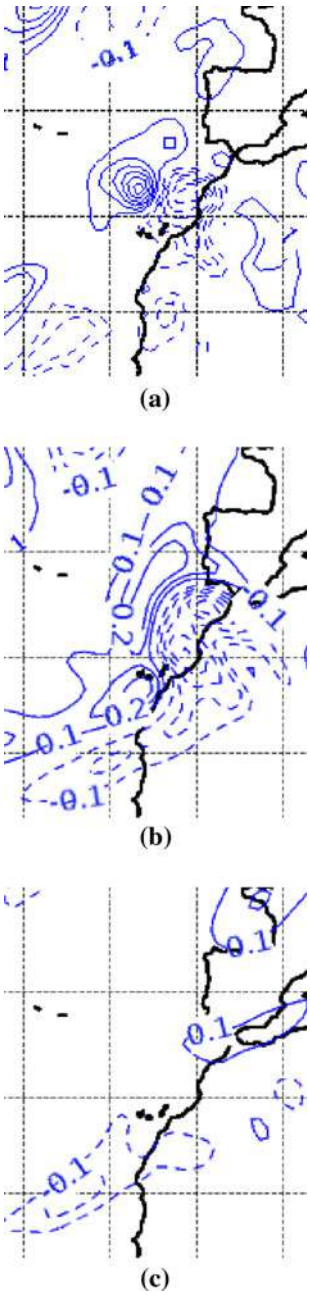

Fig. 14 500 hPa total "AB" vertical velocity (Pa s^{-1}, every 0.1 Pa s^{-1}) on 8 February 1200 UTC. Upward motion in *dashed lines* and downward motion in *solid lines*. **a** Reanalysis, **b**, **c** the 72-h reference (S1) and "modified" (S3) simulations, respectively, valid on 8 February 1200 UTC

by these authors presenting connections between PV intrusions and convection in the eastern tropical Pacific, the decrease in the static stability, together with the translational motion of the anomaly itself, results in a vertical motion in low levels. In Fig. 11, it can be noted that the ascending pole is co-located with convective clouds. Figure 14b, c presents the same field as Fig. 14a but for the 72-h ARPEGE simulations valid on 8 February 1200 UTC for the reference simulation S1 and the simulation initialized with a modified state S3, respectively. For S1 (Fig. 14b), the dipole associated with C2 is less marked (-0.5 and $+0.3$ Pa s^{-1} for upwards and downwards velocities, respectively) than with the reanalysis (Fig. 14a) but it is still present at the same location. This can be linked to the smaller deepening of the cut-off low in S1 than in the reanalyses as already mentioned. Nevertheless, the dipole is well shown for S1 whereas it is not present for S3 (Fig. 14c). The combined use of the vertical velocity diagnostics and the sensitivity test with the inversion tool shows the vertical wind dipole associated with a cut-off low. The non-formation of an ascending vertical wind core in the case of the modified simulation can be associated with the non-formation of a convective cell in the area studied. With this result, we can conclude that, in our case study, the mid-latitude Rossby wave breaking makes the environment favourable to the subtropical convective cell. This result is in agreement with those of Funatsu and Waugh (2008), which "are consistent with theoretical expectations and support the hypothesis (Kiladis 1998) that the upper level PV initiates and supports convection by destabilizing the lower troposphere and causing upward motion ahead of the tongues".

5 Conclusion

The main motivation of this study was to better understand the influence of RWB on lower level dynamics and weather forecast. A case study from 5 to 8 February 1997 has been used to investigate both a Mediterranean low and a subtropical African convective situation. This case study benefited from improved analyses from the FASTEX experiment. Using a PV inversion tool in association with the French ARPEGE model, sensitivity studies were performed. Two main results are presented. First, the Mediterranean surface low under study is shown to be associated with the mid-latitude upper level PV anomaly, itself associated with a Rossby wave. Second, a subtropical convective cell is shown to be positioned in an area made favourable to upward vertical motion associated with a cut-off low; this cut-off low coming from a mid-latitude Rossby wave.

Both cases are in agreement with theoretical expectations corresponding to the classic barocline interaction mechanism for maintaining and reinforcing a surface low (Hoskins et al. 1985) and support the Kiladis (1998) hypothesis that the upper level initiates and supports convection (Funatsu and Waugh 2008). The downstream impact of the RWB and associated physical processes are suspected to be primarily responsible for degradation in 1–7 days forecast skill in global prediction systems and their representation in numerical weather prediction

models. Many questions may arise from these studies: to what extent is it possible to generalise the downstream impact of RWB seen as a dynamical memory for Mediterranean heavy precipitation and cyclogenesis, blocking over the eastern North Atlantic and even long-range transport of Saharan dust towards Europe. It would also be interesting to better understand the role of diabatic processes, moisture, sea surface temperature in RWB.

A unique and timely opportunity for the further study on Rossby wave interactions with Mediterranean and subtropical latitudes exists within the framework of the upcoming T-NAWDEX (THORPEX-North Atlantic Waveguide and Downstream Impact Experiment) and HyMeX (Hydrological Mediterranean eXperiment) programmes.

References

Allen G, Vaughan G, Brunner D, May PT, Heyes W, Minnis P, Ayers JK (2009) Modulation of tropical convection by breaking Rossby waves. Q J R Meteorol Soc 135:125–137

Arbogast P, Maynard K, Crepin F (2008) Ertel potential vorticity inversion using a digital filter initialization method. Q J R Meteorol Soc 134:1287–1296

Argence S, Lambert D, Richard E, Chaboureau J-P, Söhne N (2008) Impact of initial condition uncertainties on the predictability of heavy rainfall in the Mediterranean: a case study. Q J R Meteorol Soc 134:1775–1788

Argence S, Lambert D, Richard E, Chaboureau J-P, Arbogast P, Maynard K (2009) Improving the numerical prediction of a cyclone in the Mediterranean by local potential vorticity modifications. Q J R Meteorol Soc 135:865–879

Basset HA, Ali AM (2006) Diagnostic of cyclogenesis using potential vorticity. Atmósfera 19(4):213–234

Bougeault P, Binder P, Buzzi A, Dirks R, Houze RA, Kuettner J, Smith RB, Steinacker R, Volkert H (2001) The MAP special observing period. Bull Am Meteorol Soc 82:433–462

Buzzi A, D'Isidoro M, Davolio S (2003) A case-study of an orographic cyclone south of the Alps during the MAP SOP. Q J R Meteorol Soc 129:1795–1818

Chaigne E, Arbogast P (2000) Multiple potential vorticity inversions in two FASTEX cyclones. Q J R Meteorol Soc 126:1711–1734

Charney JG (1947) The dynamics of long waves in a baroclinic westerly current. J Meteorol 4:135–162

Claud C, Chaboureau J-P, Argence S, Lambert D, Richard E, Gauthier N, Funatsu BM, Hauchecorne A, Arbogast P, Maynard K (2010) Impact of fine-scale upper-level structures on the deepening of a Mediterranean "hurricane". Mon Weather Rev (in revision)

Courtier P, Freyder C, Geleyn J-F, Rabier F, Rochas M (1991) The ARPEGE project at Météo-France. In: Proceedings of the ECMWF seminar on numerical methods in atmospheric models, 9–13 September 1991, vol II, pp 192–231 (available from ECMWF)

Davis CA, Emanuel KA (1991) Potential vorticity diagnostics of cyclogenesis. Mon Weather Rev 119:1929–1953

Davis-Jones R (1991) The frontogenetic forcing of secondary circulations. Part I: the duality and generalization of the Q vector. J Atmos Sci 48:497–509

Desroziers G, Pouponneau B, Thépaut JN, Janiskova M, Veersé F (1999) Four-dimensional variational analyses of FASTEX situations using special observations. Q J R Meteorol Soc 125:3339–3358

Desroziers G, Hello G, Thépaut JN (2003) A 4D-Var re-analysis of FASTEX. Q J R Meteorol Soc 129:1301–1315

Donnadille J, Cammas J-P, Mascart P, Lambert D, Gall R (2001a) A very deep tropopause fold. Part I: synoptic description and modeling. Q J R Meteorol Soc 127:2247–2268

Donnadille J, Cammas J-P, Mascart P, Lambert D (2001b) FASTEX IOP18: a very deep tropopause fold: part II: QG-omega diagnoses. Q J R Meteorol Soc 127:2269–2286

Fehlmann R, Quadri C (2000) Predictability issues of heavy alpine south-side precipitation. Meteorol Atmos Phys 72:223–231

Funatsu BM, Waugh DW (2008) Connections between potential vorticity intrusions and convection in the Eastern tropical Pacific. J Atmos Sci 65:987–1002

Hello G, Arbogast P (2004) Two different methods to correct the initial conditions applied to the storm of 27 December 1999 over southern France. Meteorol Appl 11:41–57

Hoinka KP, Richard E, Poberaj G, Busen R, Caccia JL, Fix A, Mannstein H (2003) Analysis of a potential-vorticity streamer crossing the Alps during MAP IOP 15 on 6 November 1999. Q J R Meteorol Soc 129:609–632

Holton JR (1992) An introduction to dynamic meteorology, 3rd edn. Academic Press, Dublin

Hoskins BJ, McIntyre ME, Robertson AW (1985) On the use and significance of isentropic potential vorticity maps. Q J R Meteorol Soc 111:877–946

Jiang Q, Smith RB, Doyle J (2003) The nature of the mistral: observations and modelling of two MAP events. Q J R Meteorol Soc 129:857–875

Joly A, Browning KA, Bessemoulin P, Cammas J-P, Caniaux G, Chalon J-P, Clough SA, Dirks R, Emanuel KA, Eymard L, Gall R, Hewson TD, Hildebrand PH, Jorgensen D, Lalaurette F, Langland R, Lemaître Y, Mascart P, Moore JA, Persson POG, Roux F, Shapiro MA, Snyder C, Toth Z, Wakimoto RM (1999) Overview of the field phase of the Fronts and Atlantic Storm-Track EXperiment (FASTEX) project. Q J R Meteorol Soc 125:3131–3164

Kaspar M, Müller M (2009) Cyclogenesis in the Mediterranean basin: a diagnosis using synoptic-dynamic anomalies. Nat Hazards Earth Syst Sci 9:957–965

Kiladis GN (1998) Observations of Rossby waves linked to convection over the eastern tropical Pacific. J Atmos Sci 55:321–339

Knippertz P, Martin JE (2005) Tropical plumes and extreme precipitation in subtropical and tropical West Africa. Q J R Meteorol Soc 131:2337–2365

Knippertz P, Martin JE (2007) The role of dynamic and diabatic processes in the generation of cut-off lows over Northwest Africa. Meteorol Atmos Phys 96:3–19

Kowol-Santen J, Elbern H, Ebel A (2000) Estimation of cross-tropopause airmass fluxes at midlatitudes: comparison of different numerical methods and meteorological situations. Mon Weather Rev 128:4045–4057

Krichak SO, Alpert P, Dayan M (2007) A southeastern Mediterranean PV streamer and its role in December 2001 case with torrential rains in Israel. Nat Hazards Earth Syst Sci 7:21–32

Kurz M, Dalla Fontana A (2004) A case of cyclogenesis over the western Mediterranean Sea with extraordinary convective activity. Meteorol Appl 11:97–113

Lagouvardos K, Kotroni V, Defer E (2007) The 21–22 January 2004 explosive cyclogenesis over the Aegean Sea: observations and model analysis. Q J R Meteorol Soc 133:1519–1531

Lambert D, Arbogast P, Cammas J-P, Donnadille J, Mascart P (2004) A cold air cyclogenesis study using potential vorticity inversion method. Q J R Meteorol Soc 130:2953–2970

Lanzinger A (1992) Upper and lower level PV-coupling associated with Alpine lee cyclogenesis. Meteorol Z 1:173–181

Lebeaupin C, Ducrocq V, Giordani H (2006) Sensitivity of torrential rain events to the sea surface temperature based on high-resolution numerical forecasts. J Geophys Res 111:D12110. doi: 10.1029/2005JD006541

Liniger MA, Davies HC (2003) Substructure of a MAP streamer. Q J R Meteorol Soc 129:633–651

Mallet I, Cammas J-P, Mascart P, Bechtold P (1999) Effects of cloud diabatic heating on a FASTEX cyclone (IOP 17) early development. Q J R Meteorol Soc 125:3415–3438

Massacand AC, Wernli H, Davies HC (1998) Heavy precipitation on the Alpine southside: an upper-level precursor. Geophys Res Lett 25:1435–1438

Massacand AC, Wernli H, Davies HC (2001) Influence of upstream diabatic heating upon an Alpine event of heavy precipitation. Mon Weather Rev 129:2822–2828

McIntyre ME, Palmer TN (1983) Breaking planetary waves in the stratosphere. Nature 305:593–600

McTaggart-Cowan R, Gyakum JR, Yau MK (2003) Moist component potential vorticity. J Atmos Sci 60:166–177

Moore RW, Montgomery MT, Davies HC (2008a) The integral role of a diabatic Rossby Vortex in a heavy snowfall event. Mon Weather Rev 136:1878–1897

Moore RW, Martius O, Davies HC (2008b) Downstream development and Kona low genesis. Geophys Res Lett 35:L20814. doi: 10.1029/2008GL035502

Porcù F, Carrassi A, Medaglia CM, Prodi F, Mugnai A (2007) A study on cut-off low vertical structure and precipitation in the Mediterranean region. Meteorol Atmos Phys 96:121–140

Postel GA, Hitchman MH (1999) A climatology of Rossby wave breaking along the subtropical tropopause. J Atmos Sci 56:359–373

Prezerakos NG, Flocas HA, Michaelides SC (1999) Upper-tropospheric downstream development leading to surface cyclogenesis in the central Mediterranean. Meteorol Appl 6:313–322

Stull RB (2000) Meteorology for scientists and engineers, 2nd edn. Brooks-Cole, Belmont